

# Increasing the Resistance of Living Cells Against Oxidative Stress by Non-Natural Surfactants as Membrane Guards

*Marius Kunkel, Stefan Schildknecht, Klaus Boldt, Lukas Zeyffert, David Schleheck, Marcel  
Leist and Sebastian Polarz\**

University of Konstanz, Universitätsstrasse 10, 78457 Konstanz, Germany

## **Corresponding Author**

\*E-mail: [sebastian.polarz@uni-konstanz.de](mailto:sebastian.polarz@uni-konstanz.de).

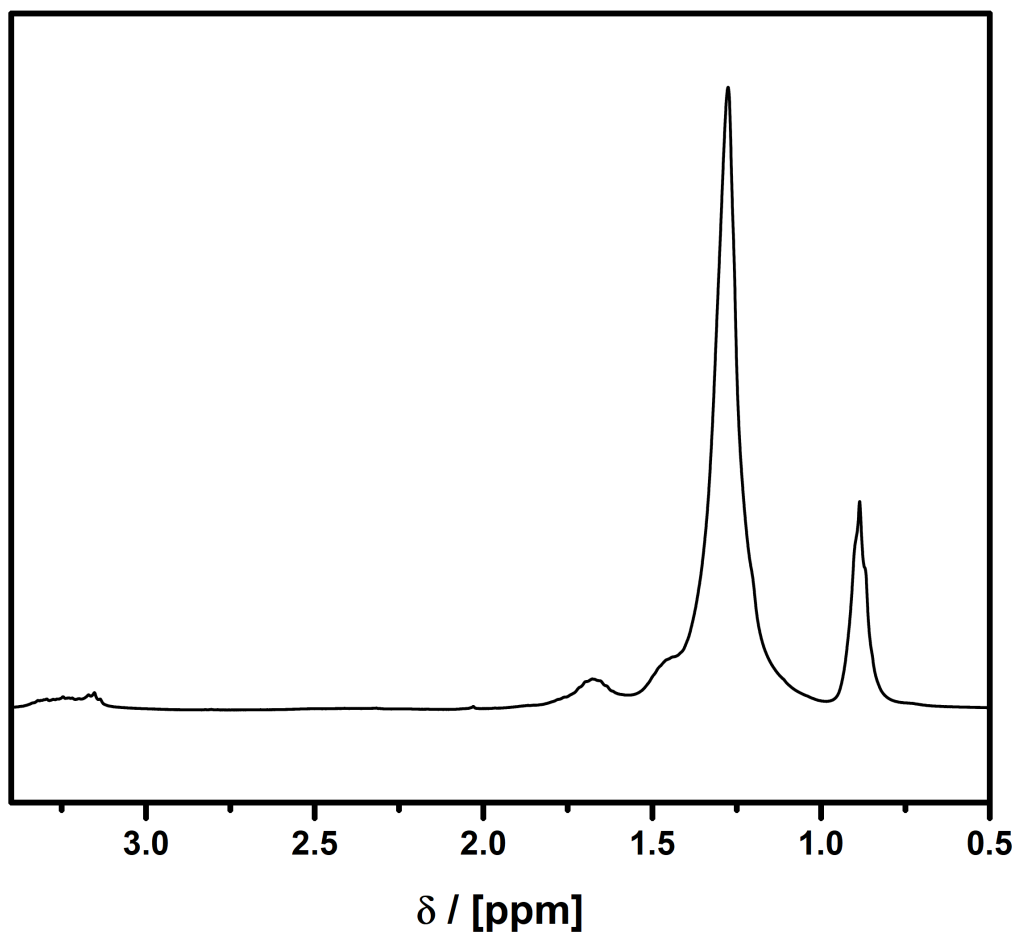


**Fig. S1.**  $^1\text{H-NMR}$  for compound (**3**) in  $\text{CDCl}_3$ .  $^1\text{H-NMR}$  (400 MHz,  $\text{CDCl}_3$ ):  $\delta(\text{ppm}) = 0.89$  (t,  $3J = 7.2$  Hz, 15 H), 1.27 (m, 90 H), 1.45 (m, 10 H), 1.67 (m, 10 H), 3.22 (m, 5 H)

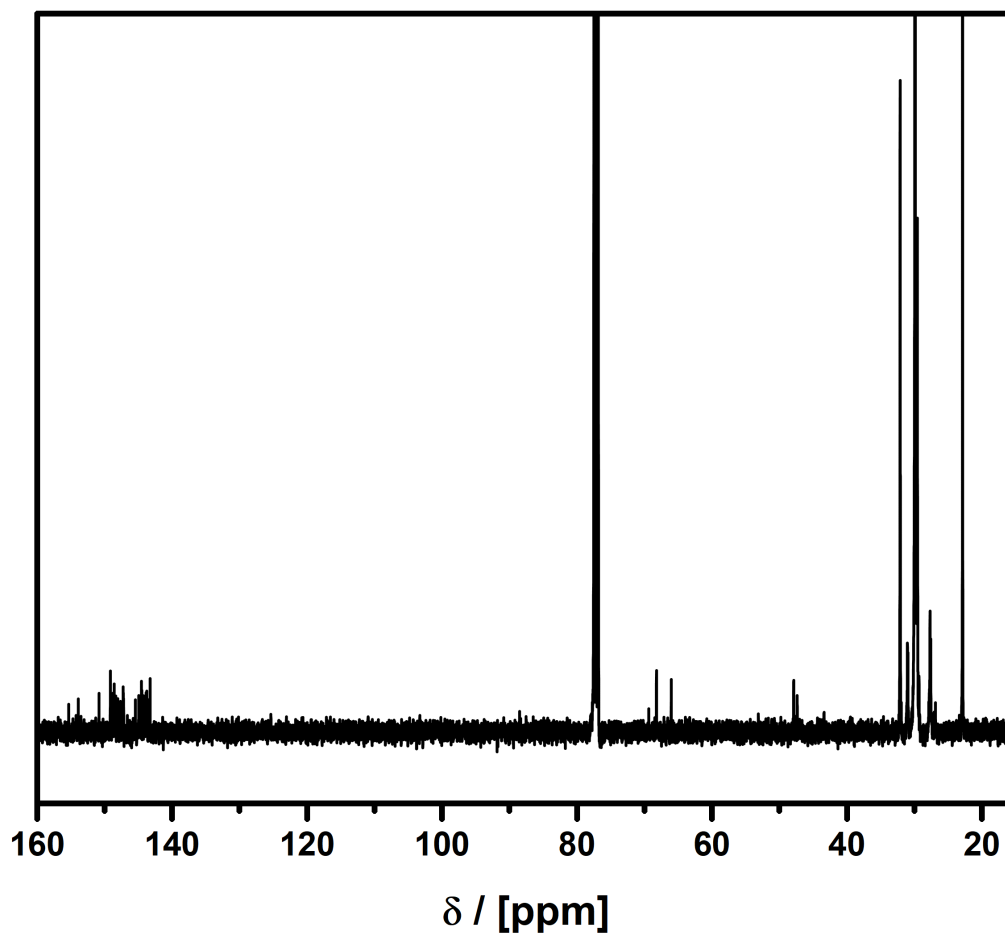


**Fig. S2.**  $^{13}\text{C}$ -NMR for compound (**3**) in  $\text{CDCl}_3$ .  $^{13}\text{C}$ -NMR (100 MHz,  $\text{CDCl}_3$ ):  $\delta$ (ppm) = 22.56, 27.57, 27.67, 29.56, 29.58, 29.91, 29.93, 30.95, 31.02, 32.11, 47.36, 47.87, 47.88, 66.02, 68.21, 69.35, 143.24, 143.31, 143.71, 143.81, 143.83, 143.84, 143.84, 143.88, 144.02, 144.08, 144.31, 144.47, 144.51, 144.53, 144.91, 145.43, 147.16, 147.21, 147.23, 147.29, 147.62, 148.02, 148.21, 148.33, 148.57, 148.71, 149.12, 150.81, 153.88, 155.31

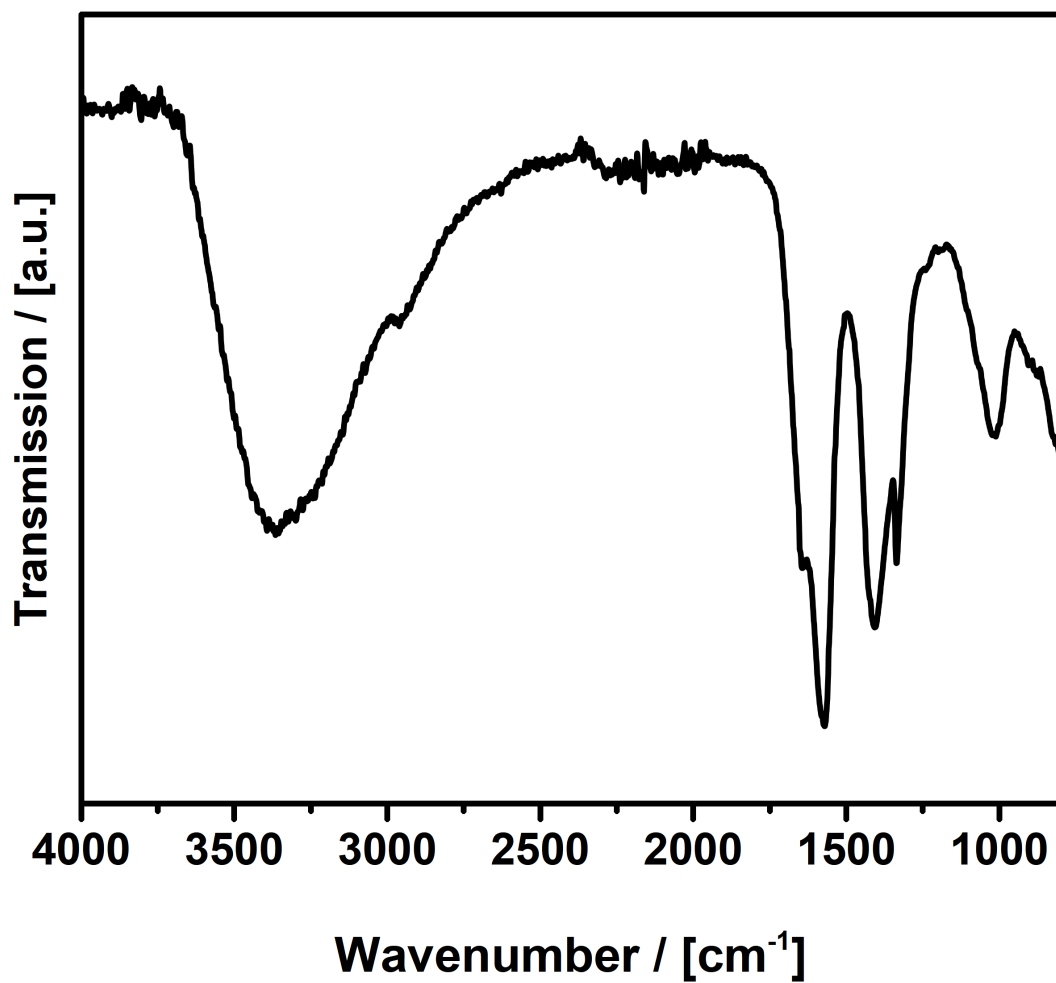


**Fig. S3.** FT-IR for compound (**4cc**). ATR-IR:  $\nu$  (cm<sup>-1</sup>) = 3365, 2942, 2971, 1645, 1574, 1409, 1325, 1032.

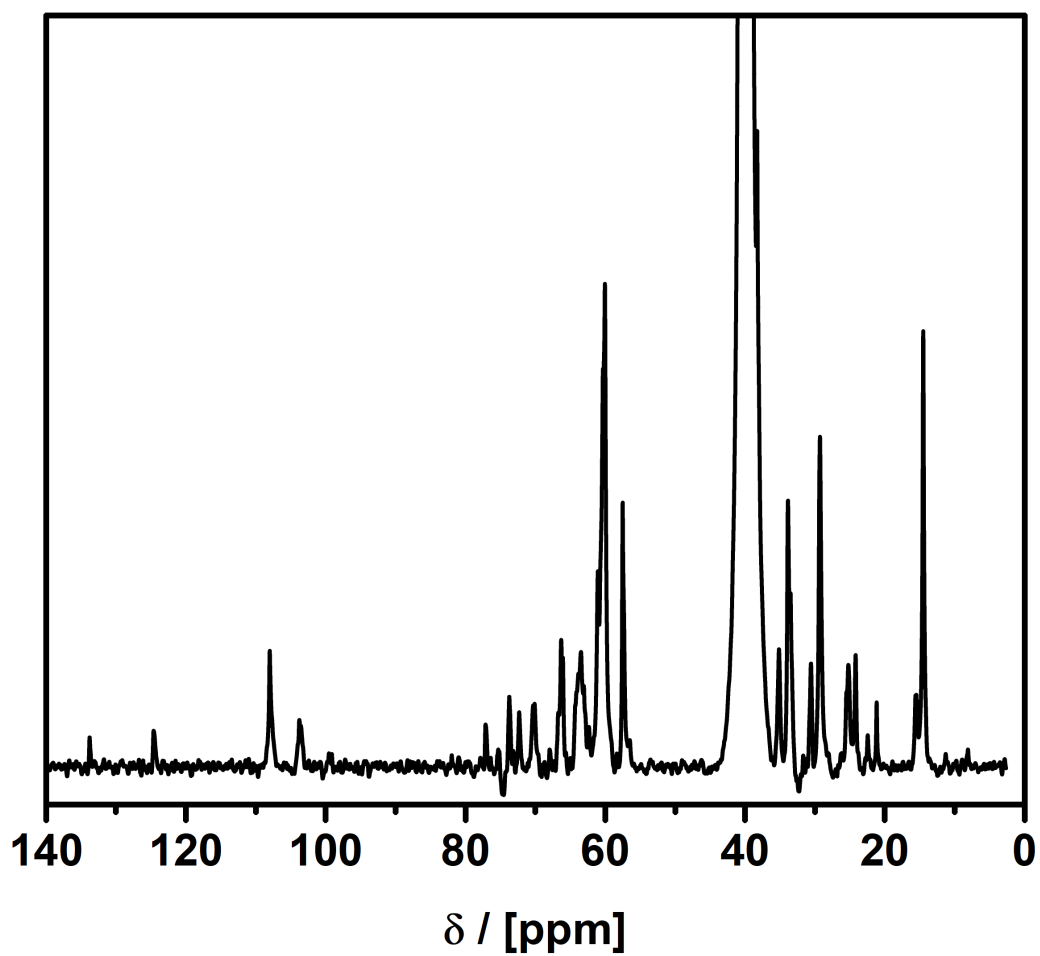


**Fig. S4.**  $^{13}\text{C}$ -NMR for compound (**4cc**) in  $\text{D}_2\text{O}$ .  $^{13}\text{C}$ -NMR (100 MHz,  $\text{D}_2\text{O}$ ):  $\delta(\text{ppm}) = 13.26, 16.81, 20.39, 20.53, 23.23, 23.34, 27.93, 28.77, 30.35, 30.65, 33.24, 33.33, 36.722, 36.84, 36.85, 52.42, 57.26, 57.28, 60.52, 60.59, 60.76, 60.84, 61.73, 64.45, 174.16, 174.48$ .

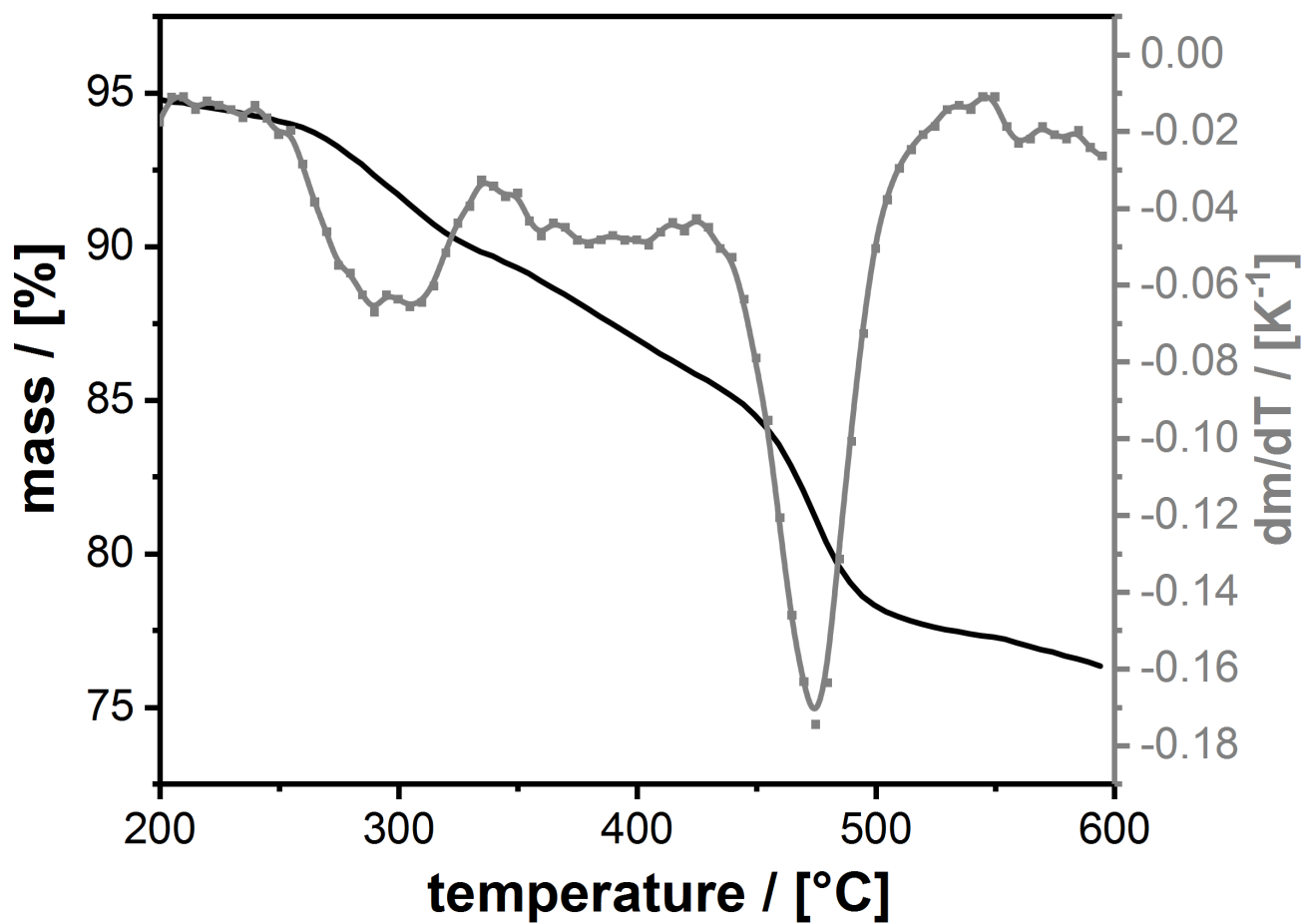


**Fig. S5.** TGA for compound (4cc) under inert conditions (N<sub>2</sub> atmosphere). step: 5.91 %, 2. step: 17.05 %. The number of OH-groups was among others determined by TGA (N<sub>2</sub>, 1 K/min).

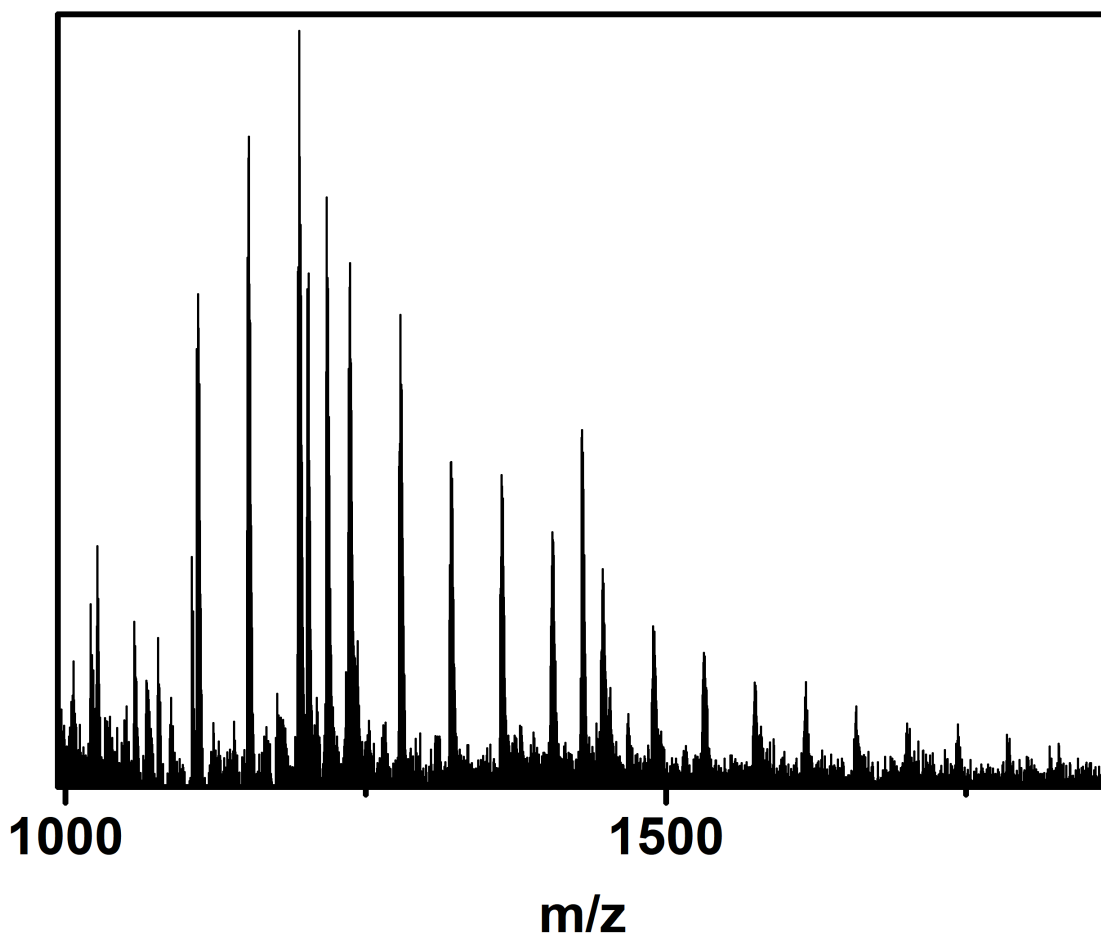


**Fig. S6.** MALDI-MS for compound (4cc). 1615  $[\text{HC}_{60}(\text{HNC}_{12}\text{H}_{25})_3(\text{OH})_{20}]^+$ , 1827.1  
 $[\text{HC}_{60}(\text{HNC}_{12}\text{H}_{25})_5(\text{OH})_8(\text{O})_3]^+$ , 1741.7  $[\text{HC}_{60}(\text{HNC}_{12}\text{H}_{25})_4(\text{OH})_{12}(\text{O})_4(\text{NH})]^+$ , 1656.8  
 $[\text{HC}_{60}(\text{HNC}_{12}\text{H}_{25})_4(\text{OH})_7(\text{O})_4\text{NH}]^+$ , 1615  $[\text{HC}_{60}(\text{HNC}_{12}\text{H}_{25})_3(\text{OH})_{20}]^+$ , 1573.6  
 $[\text{HC}_{60}(\text{HNC}_{12}\text{H}_{25})_3(\text{HN})_2(\text{OH})_{13}(\text{O})_3]^+$ , 1529.6  $[\text{HC}_{60}(\text{HNC}_{12}\text{H}_{25})_3(\text{OH})_{15}]^+$ , 1488.6  
 $[\text{HC}_{60}(\text{HNC}_{12}\text{H}_{25})_3(\text{NH})(\text{OH})_7(\text{O})_5]^+$ , 1446.9  $[\text{HC}_{60}(\text{HNC}_{12}\text{H}_{25})_2(\text{OH})_{21}]^+$ , 1429.8  
 $[\text{HC}_{60}(\text{HNC}_{12}\text{H}_{25})_2(\text{OH})_{20}]^+$ , 1404.2  $[\text{HC}_{60}(\text{HNC}_{12}\text{H}_{25})_2(\text{HN})_2(\text{OH})_{13}(\text{O})_4]^+$ , 1361.5  
 $[\text{HC}_{60}(\text{HNC}_{12}\text{H}_{25})_2(\text{OH})_{16}]^+$ , 1319.9  $[\text{HC}_{60}(\text{HNC}_{12}\text{H}_{25})_2(\text{HN})_3(\text{OH})_9(\text{O})_2]^+$ , 1277.8  
 $[\text{HC}_{60}(\text{HNC}_{12}\text{H}_{25})_2(\text{OH})_{11}]^+$ , 1235.8  $[\text{HC}_{60}(\text{HNC}_{12}\text{H}_{25})_1(\text{HN})_3(\text{OH})_{13}\text{O}_4]^+$ , 1217.3  
 $[\text{HC}_{60}(\text{HNC}_{12}\text{H}_{25})_1(\text{HN})_3(\text{OH})_{11}\text{O}_5]^+$ , 1201.3  $[\text{HC}_{60}(\text{HNC}_{12}\text{H}_{25})_1(\text{HN})_3(\text{OH})_{11}\text{O}_4]^+$ , 1193.7  
 $[\text{HC}_{60}(\text{HNC}_{12}\text{H}_{25})_1(\text{OH})_{16}\text{O}]^+$ , 1151.5  $[\text{HC}_{60}(\text{HNC}_{12}\text{H}_{25})_1(\text{HN})_2(\text{OH})_8(\text{O})_5]^+$ , 1109.4  
 $[\text{HC}_{60}(\text{HNC}_{12}\text{H}_{25})_1(\text{OH})_{12}]^+$ , 1026.3  $[\text{HC}_{60}(\text{OH})_{17}(\text{O})]^+$

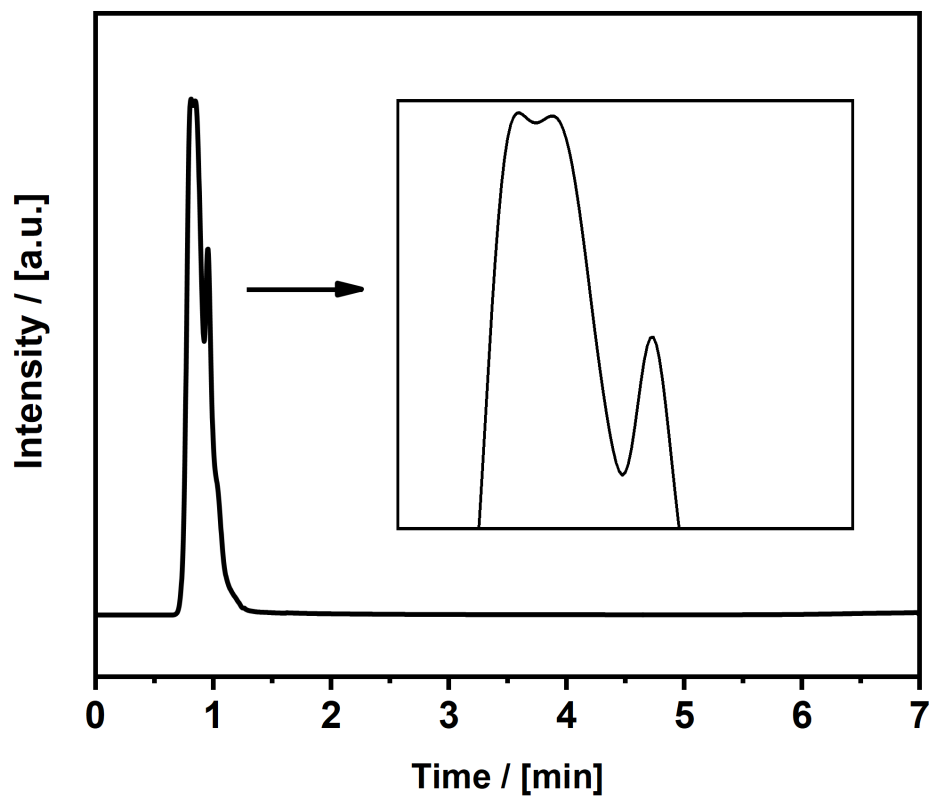


**Fig. S7.** Chromatogram of (**4cc**). 5% MeCN as eluent A and 95% water as eluent B with 0.1 % formic acid. A linear gradient of 5% A to 100% A was applied with a flow rate of 0.3 mL/min.



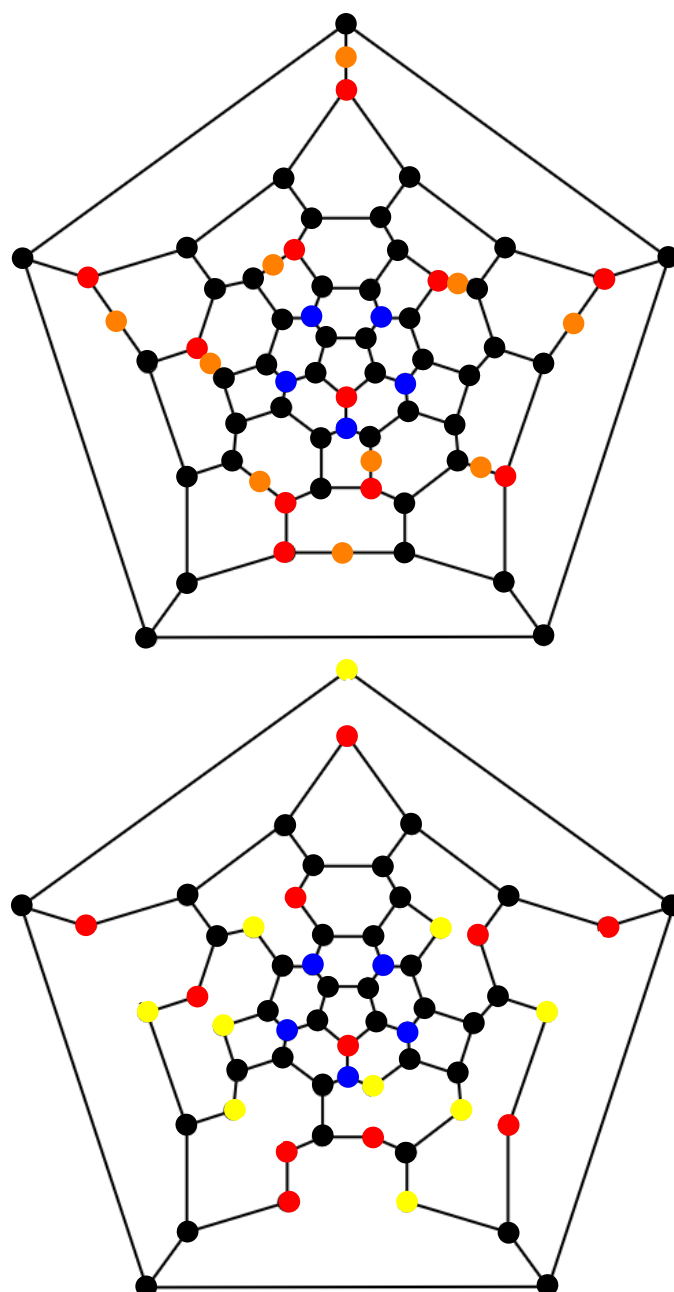


**Fig. S8.** Schematic Schlegel diagrams of one possible structure for the fulleranol surfactant systems. Top hemiketal structure (**4cc**), bottom ketone enriched structure (**4oc**). Red: C-OH, orange: -O-, yellow: C=O, blue: C-NHR.

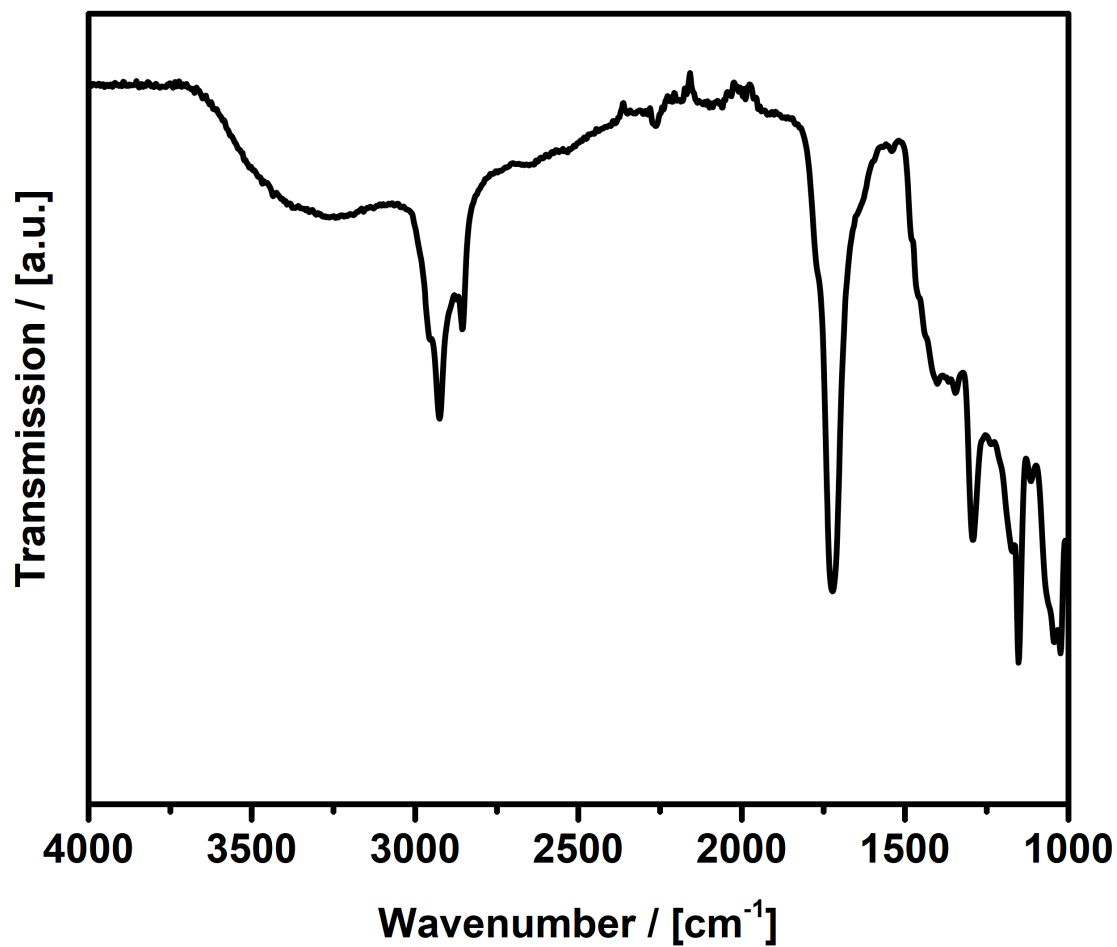


**Fig. S9.** Conversion of (**4cc**) to (**4oc**). ATR-IR:  $\nu$  (cm<sup>-1</sup>) = 3600-2364, 2971, 2942, 1720, 1623, 1396, 1155, 1023.

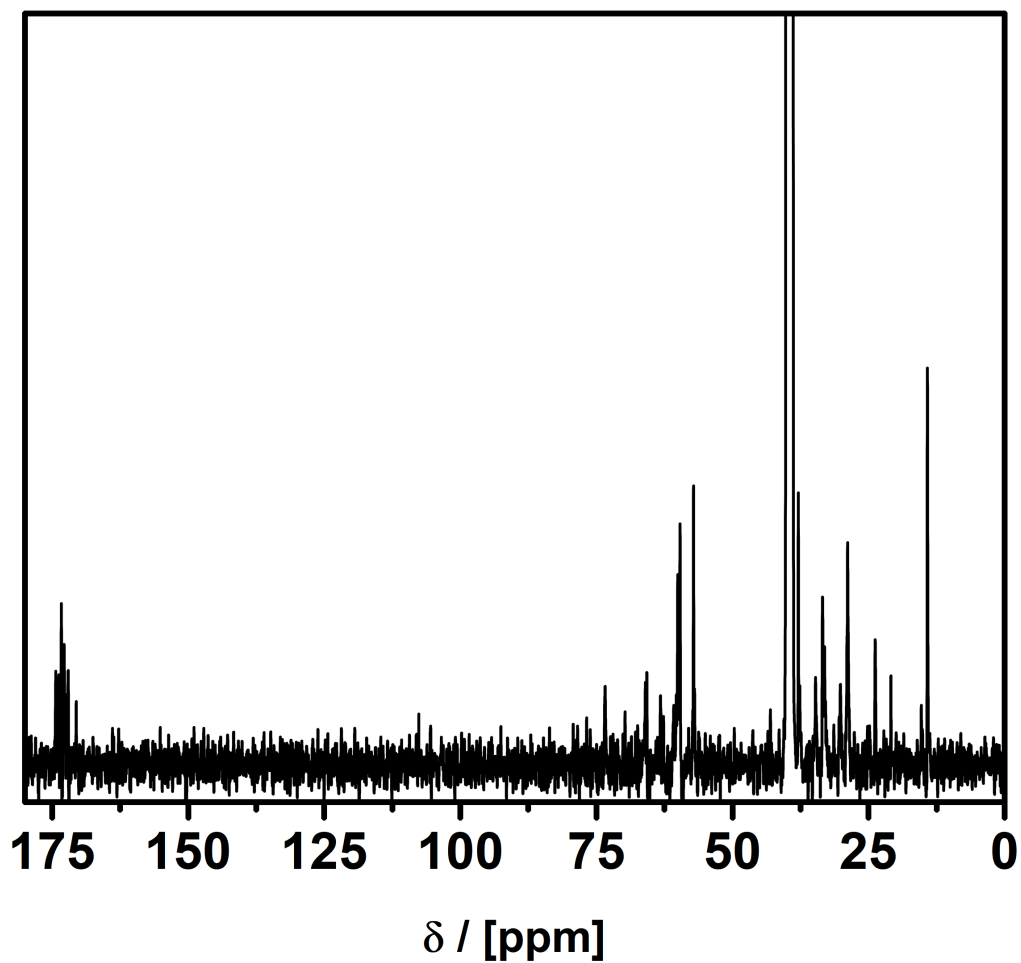


**Fig. S10.**  $^{13}\text{C}$ -NMR compound open cage (**4oc**) in  $\text{DMSO-}d_6$ .  $^{13}\text{C}$ -NMR (100 MHz,  $\text{DMSO}$ ):  $\delta$ (ppm) = 14.18, 20.89, 23.78, 28.84, 28.89, 30.18, 32.88, 33.07, 33.45, 34.74, 37.63, 37.89, 37.91, 60.31, 60.78, 62.65, 63.21, 65.72, 65.77, 65.98, 69.73, 73.39, 114.32, 170.54, 172.02, 172.27, 172.62, 172.76, 173.27, 173.52, 173.73, 174.29, 174.33.

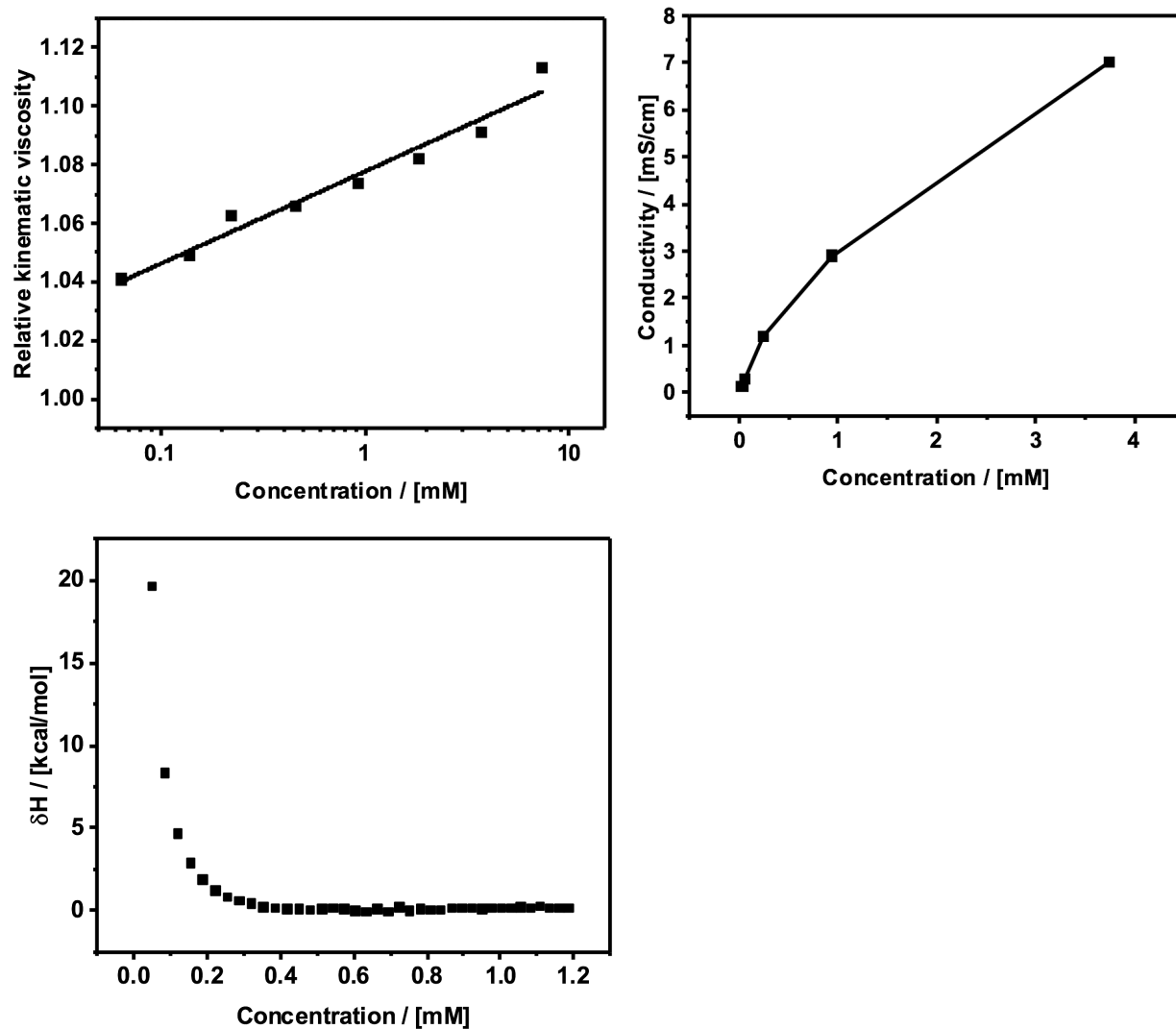
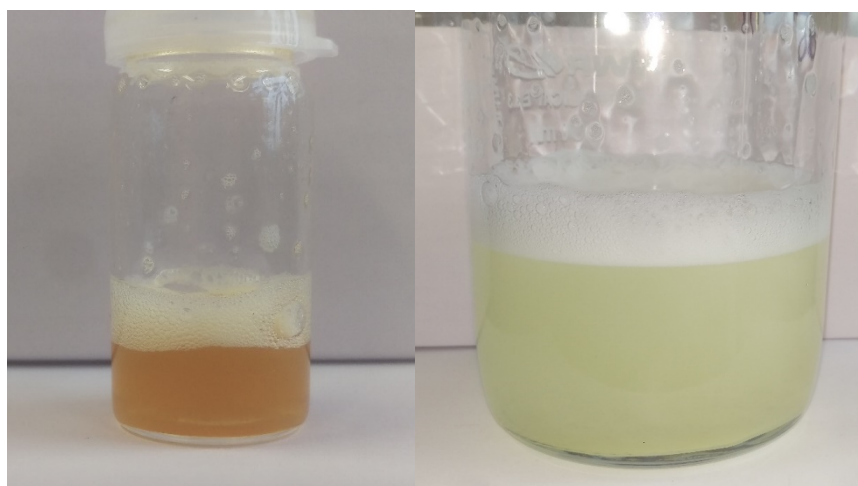
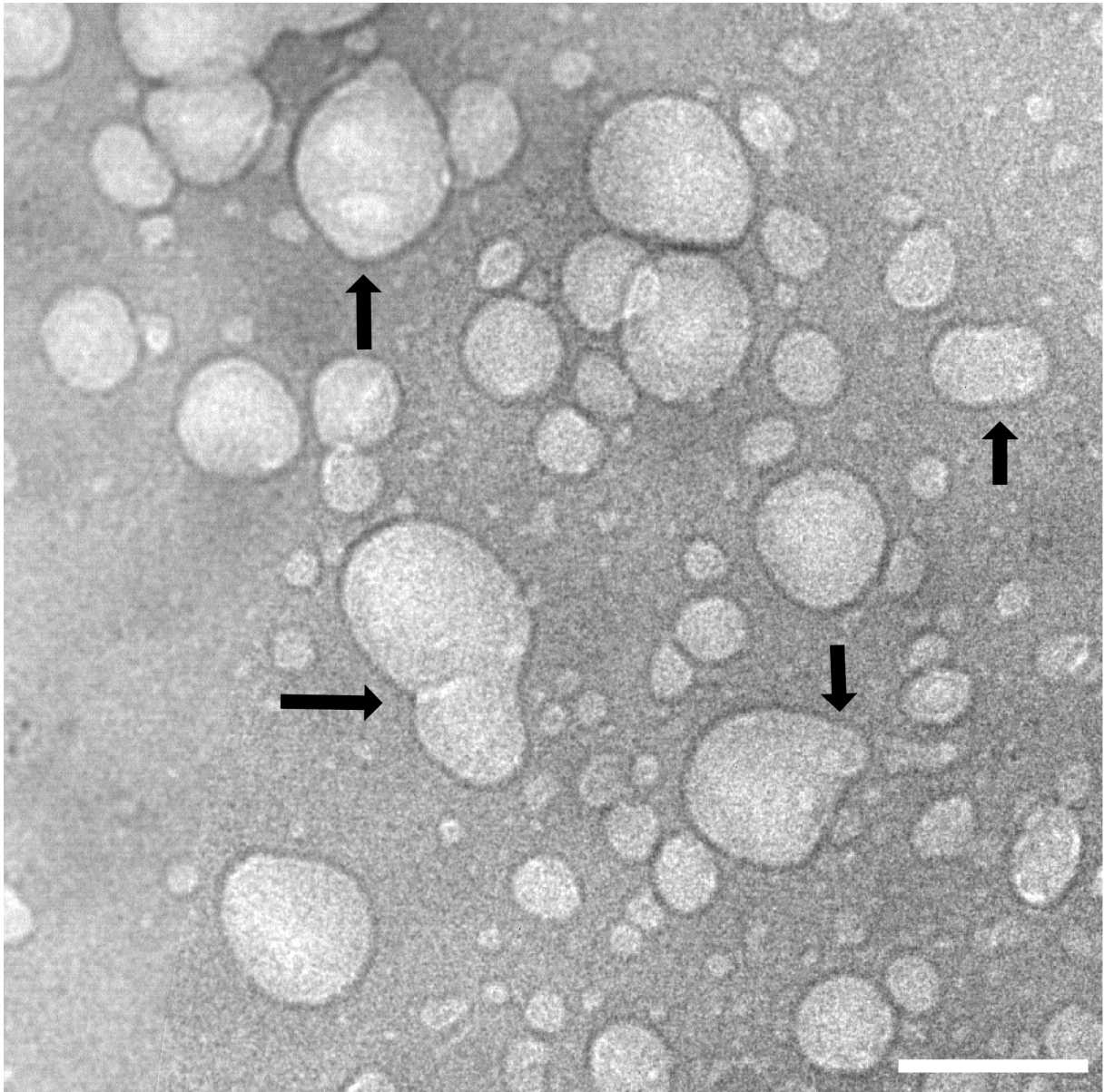


**Fig. S11.** Top left: Relative viscosity measurement of (**4cc**) in Milli-Q at rt. Top right: Conductivity (ionic) of (**4**) in Milli-Q at rt. Bottom: Isothermal titration calorimetry (ITC) of (**4**) in Milli-Q. A discontinuous relation between concentration and the observable parameter (viscosity, conductivity, or ITC signal) would indicate a change in the aggregation state of the system, respectively the occurrence of aggregation/ micellization. Obviously, all curves are continuous. A classic cmc cannot be identified.

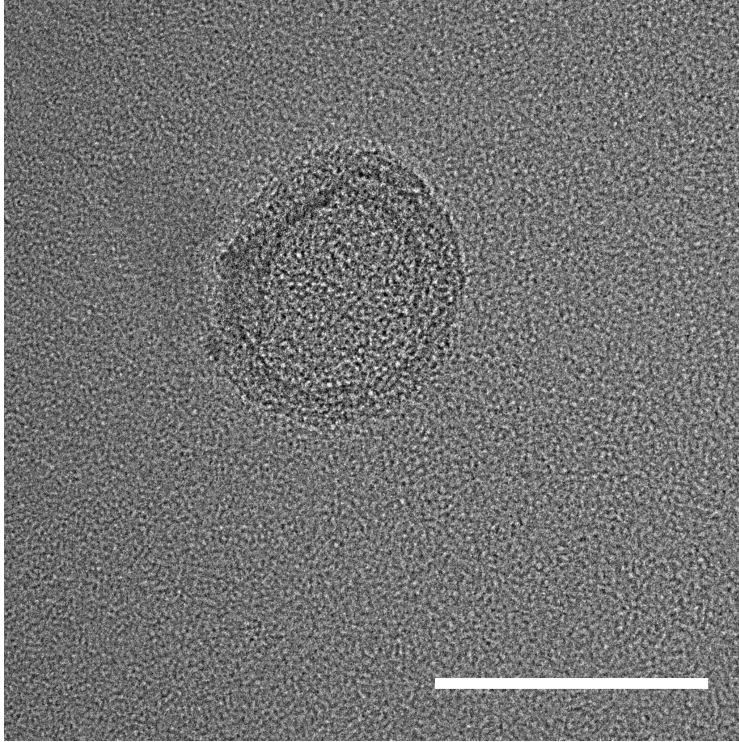
**Fig. S12.** Additional data for aggregate dispersions in water.



(a) Dispersions of (**4cc**; left) and (**4oc**; right) in water at oversaturated concentration.



(b) Additional TEM micrograph, scalebar = 100 nm. Arrows indicate positions, where vesicles have started to fuse.



(c) Additional TEM micrograph, scalebar = 50 nm.

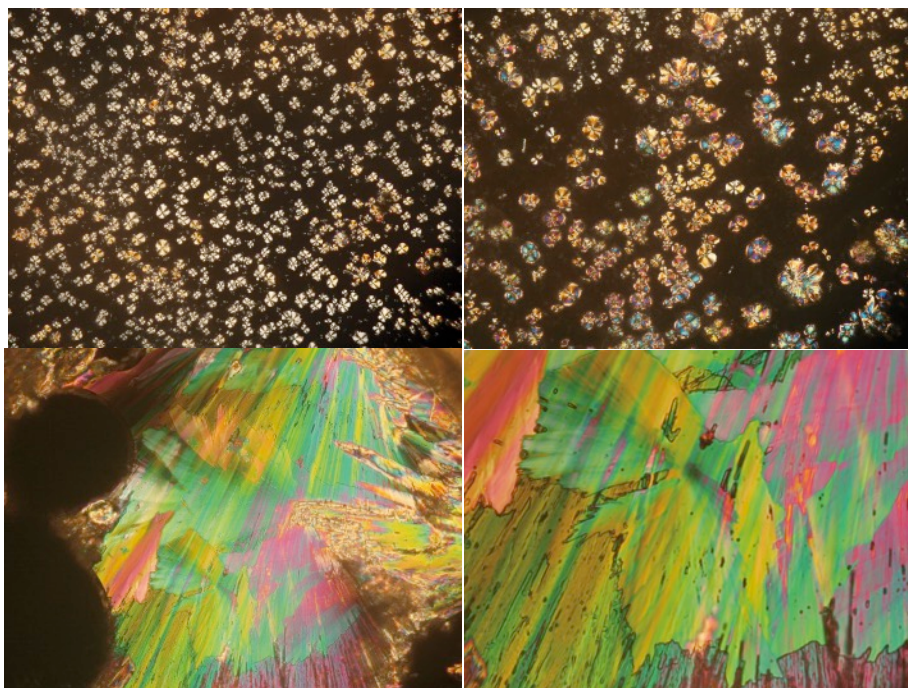


**Fig. S13.** Optical polarization microscopy image of columnar super structures of (**4cc**) with characteristic Maltese crosses (top) and smectic phase of (**4cc**) (bottom). In dependence of the surfactant concentration and grow time, one observes columnar droplets and extended birefringent areas. The columnar droplets show the classic Maltese cross pattern indicating a 360 ° rotation in optic axis orientation. The extended birefringent areas imply lamellar packing.<sup>1-2</sup>



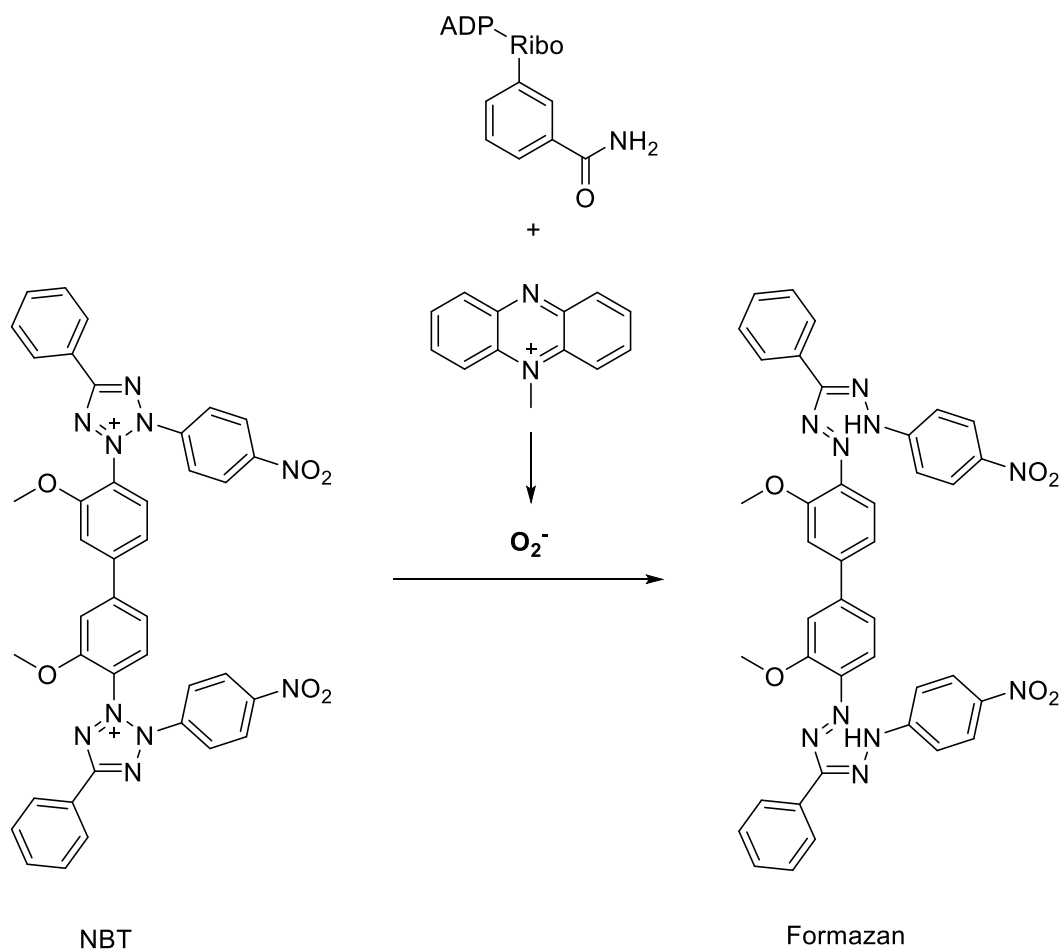


**Fig. S14.** Nitroblue tetrazolium assay.<sup>3</sup> The NBT-assay was performed after a standard procedure. 1 mL reaction mixture contained phosphate buffer (20 mM, pH 7.4), NADH (146  $\mu$ M), NBT (100  $\mu$ M), PMS (30  $\mu$ M) and various concentrations of sample solution. After incubation for 5 min at ambient temperature, the absorbance was taken at 560 nm against an appropriate blank solution. All tests were performed at least 3 times. For the quercetin experiment methanolic solutions were used.

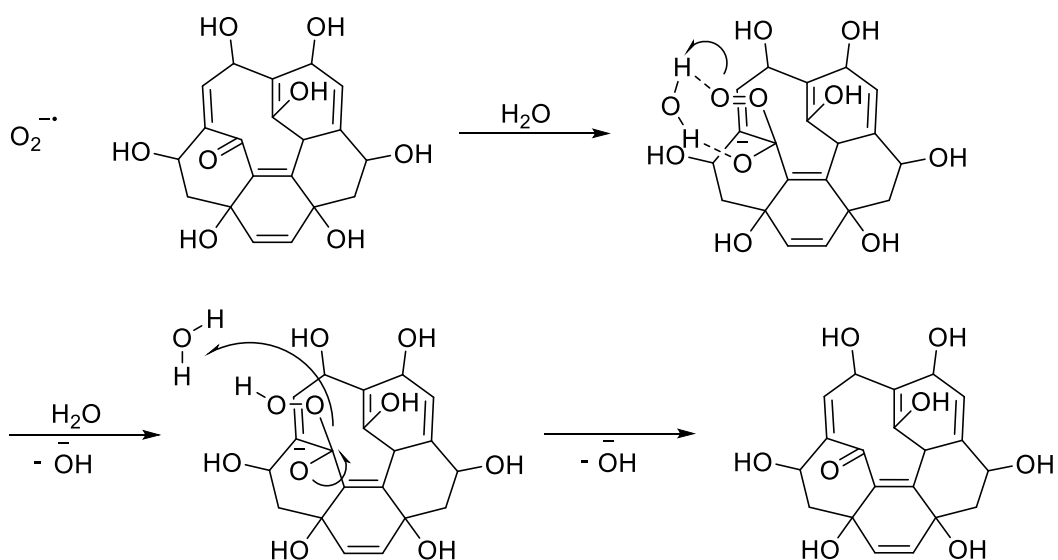


**Fig. S15.** Molecular mechanism for the improved ROS quenching activity of the open form. Additionally, to the classic superoxide quenching mechanism of fulleranol, in which the superoxide coordinates to the remaining double bonds, one can assume a mechanism in which the superoxide directly reacts with a ketone moiety. This mechanism might be reversible.

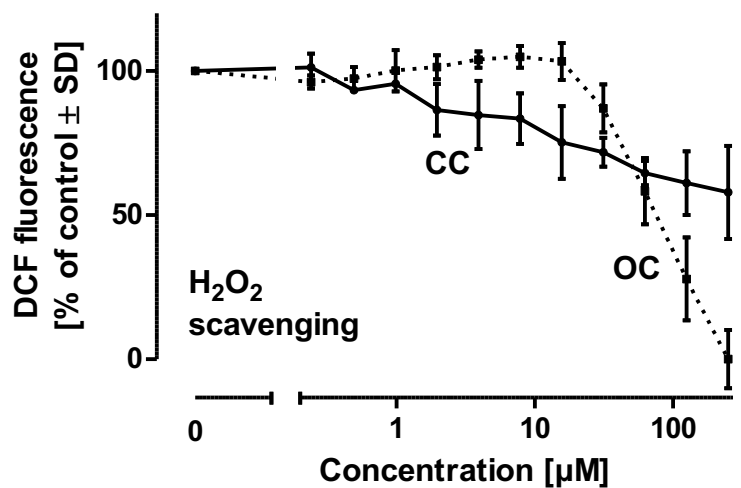
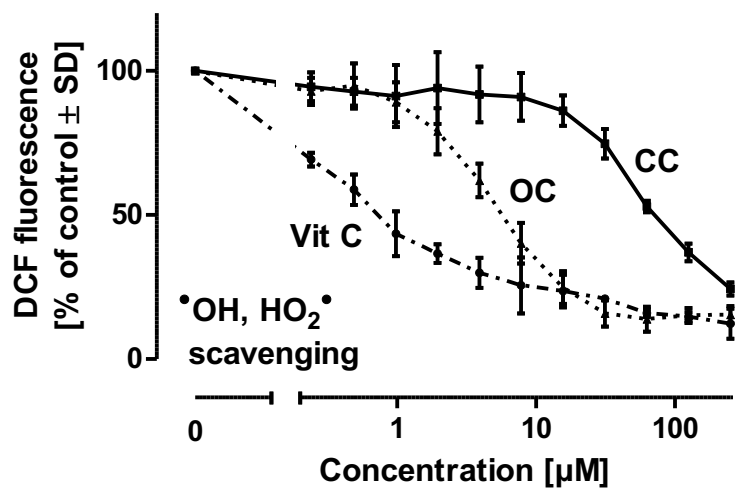
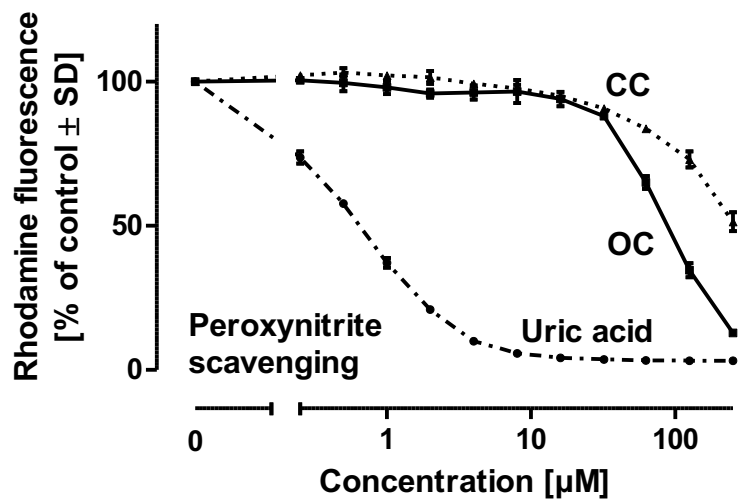
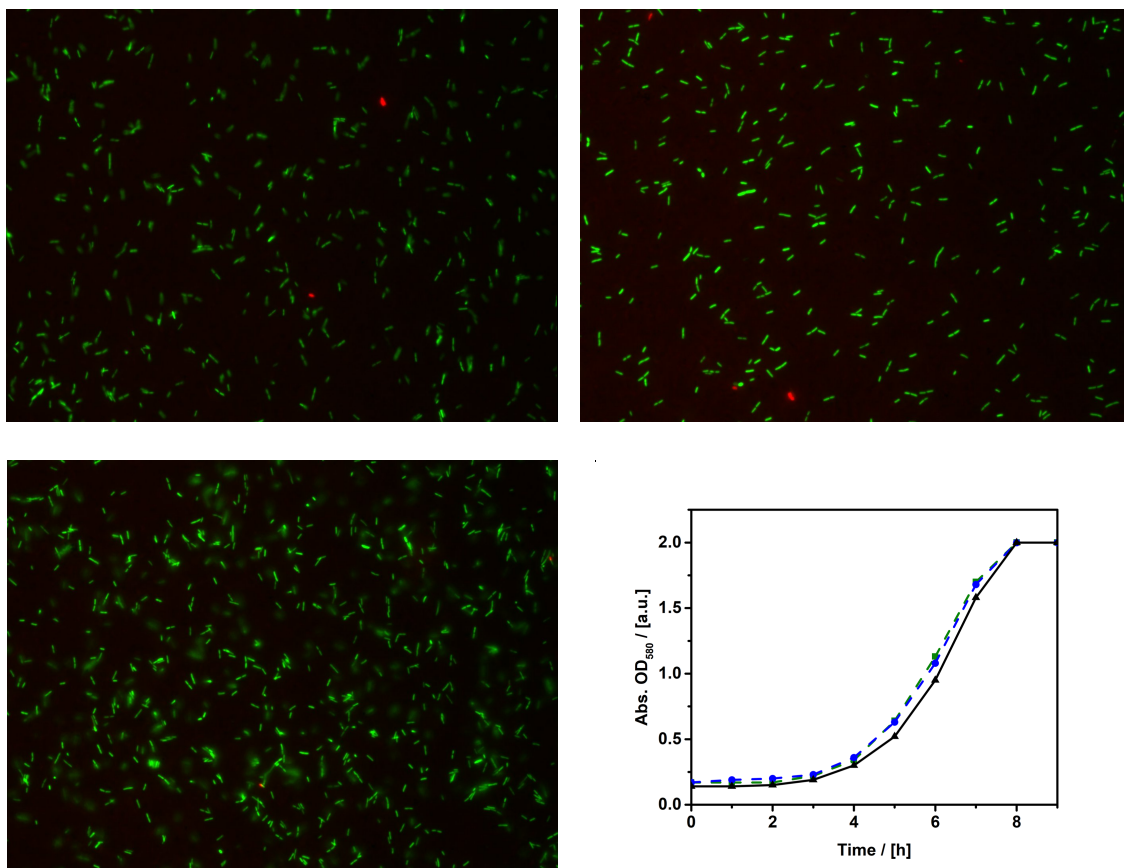
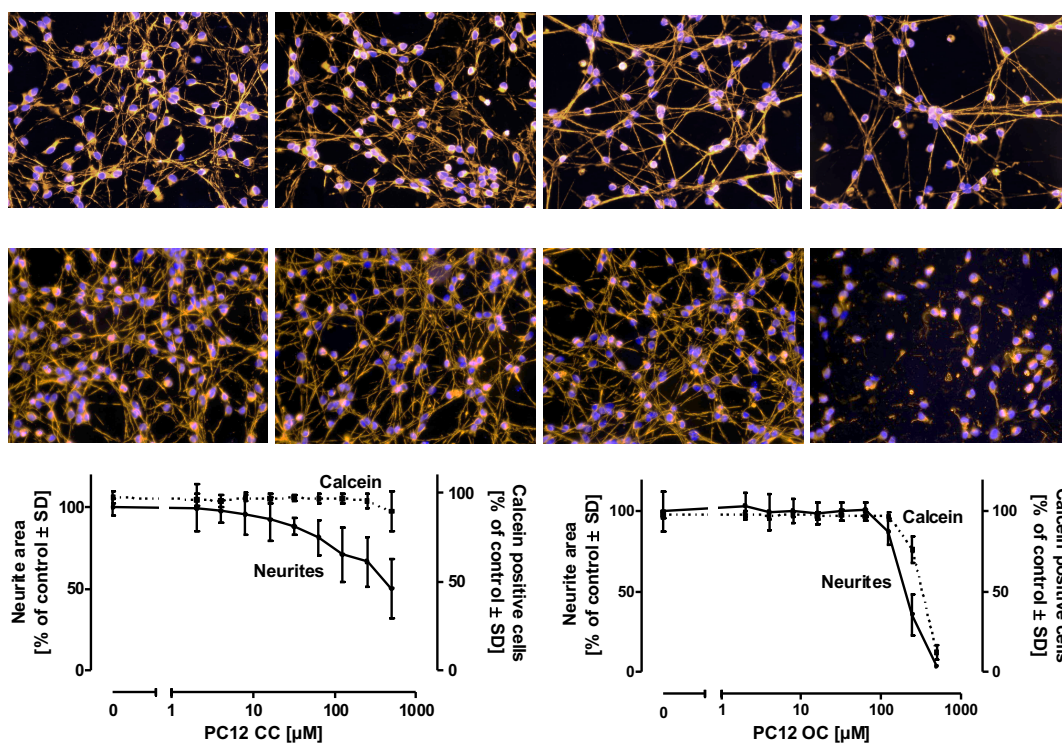


Fig. S16. ROS quenching assays for peroxynitrite, hydroxyl radicals and hydrogen peroxide<sup>4</sup>



**Fig. S17.** Live-Dead stain and growth for *E.coli* treated with surfactant . Top left control, top right, in the presence of 100  $\mu\text{M}$  of (**4cc**), bottom left, in the presence of 100  $\mu\text{M}$  of (**4oc**), bottom right growth curves with the control culture indicated in blue, the culture with (**4**) green, and the culture with the open cage isomer of (**4**) in black.

*E.coli* K-12 as well as *P. aeruginosa* PAO1 (data not shown) was inoculated from precultures into 3 mL LB-medium (10 g tryptone, 5 g yeast extract, 5 g NaCl per liter) and incubated at 30 °C. The surfactant was tested from 1  $\mu\text{M}$  up to 100  $\mu\text{M}$ . The growth of the cultures was followed by measuring the optical density (OD 580 nm), and during the growth and in the stationary phase, samples were taken. For live-dead staining when following the manufacturer's instructions (LIVE/DEAD BaCLight Bacterial Viability Kit, Thermofisher), it stains cells with membrane damage in red, against viable cells stained in green. The stained cells were placed on agar-coated microscope slides and observed under a fluorescence microscope at 400-fold magnification.



**Fig. S18.** Morphology of LUHMES treated with (**4cc**) (top), with (**4oc**) (mid) and quantification of the assay (bot) (0  $\mu\text{M}$ , 32  $\mu\text{M}$ , 125  $\mu\text{M}$ , 500  $\mu\text{M}$ ). **Cell culture:** LUHMES cells are conditionally immortalized human fetal ventral mesencephalic neuronal precursor cells with a distinct dopaminergic phenotype, described in detail previously.<sup>5-6</sup> Cell culture plates (Sarstedt) were coated with 50  $\mu\text{g}/\text{ml}$  poly-L-ornithine (PLO) and 1  $\mu\text{g}/\text{ml}$  fibronectin over night at 37°C and washed 2 times with water. Cells were propagated in Advanced DMEM/F12 (Gibco/Invitrogen, Darmstadt, Germany), 1x N2 supplement (Invitrogen), 2 mM L-glutamine (Gibco), and 40 ng/ml recombinant bFGF (R+D Systems; Minneapolis, MN). The differentiation process was initiated by addition of differentiation medium consisting of advanced DMEM/F12, 1x N2 supplement, 2 mM L-glutamine, 1 mM dibutyryl-cAMP (Sigma), 1  $\mu\text{g}/\text{ml}$  tetracycline (Sigma), and 2 ng/ml recombinant human GDNF (R+D Systems). After 2 days, cells were trypsinized and collected in Advanced DMEM/F12 medium. Cells were seeded onto 96-well plates at a density of 35.000 cells/well. The differentiation process was continued for additional 3 days, the cells were then treated with the respective compounds for an additional period of 48 h. For visualization of cell morphology, cells were fixed with 4% paraformaldehyde for 20 min at RT, permeabilized with 0.2% Triton X-100, washed, and blocked with 1% BSA (Calbiochem, San Diego, CA) in PBS for 1 h. LUHMES were stained with an anti- $\beta$ -III-tubulin antibody (rabbit, Sigma, 1:1000) in 1% BSA/PBS at 4°C over night. After washing, the secondary antibodies were added for 1 h, nuclei were stained by Hoechst H-33342 (1  $\mu\text{g}/\text{ml}$ ) for 20 min. For quantitative evaluation of the neurite area, live staining of LUHMES was conducted with Calcein-AM (1  $\mu\text{M}$ ) and Hoechst H-33342 (1  $\mu\text{g}/\text{ml}$ ) for 30 min. Images were collected by an automated microplate-reading microscope (Array-Scan II<sup>®</sup> HCS Reader, Cellomics, Pittsburgh, PA) equipped with a Hamamatsu ORCA-ER camera (resoluutuion 1024 x 1024; run at 2 x 2 binning) in two different fluorescence channels. Nuclei were identified as objects according to their intensity, size, area and shape. A virtual area corresponding to the cell soma was defined around each nucleus. The total Calcein pixel area per field minus the soma areas in that field was defined as neurite mass. In addition, viability was analyzed by the detection of the percentage of those cells positive for Calcein and for H-33342.

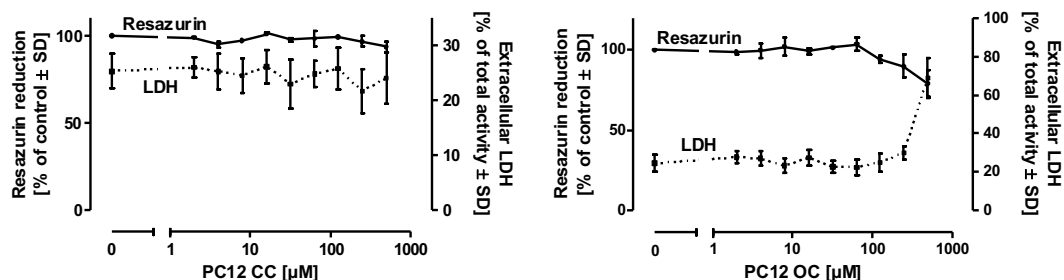


**Fig. S19.** Resazurin metabolization assay and Lactate dehydrogenase (LDH) release assay for the treatment of LUHMES with (**4cc**) (left) and (**4oc**) (right).

Resazurin metabolization assay: Resazurin (Sigma) was added to the cell culture medium in a final concentration of 5 μg/ml, fluorescence was measured after 60 min ( $\lambda_{ex}=530$  nm;  $\lambda_{em}=590$  nm). Lactate dehydrogenase (LDH) release assay: LDH activity was detected separately in the supernatant and cell lysate. Following separation of the supernatants, cells were lysed in PBS / 0.5% Triton X-100 for > 60 min. The percentage of LDH released was calculated as  $100 \times \text{LDH}_{\text{supernatant}} / \text{LDH}_{\text{supernatant} + \text{lysate}}$ . For the enzymatic assay, 20 μl of sample was combined with 180 μl of reaction buffer containing NADH (100 μM) and sodium pyruvate (600 μM) in sodium phosphate buffer adjusted to pH 7.4 by titration with  $\text{K}_2\text{HPO}_4$  (40 mM) and  $\text{KH}_2\text{PO}_4$  (10 mM). Absorption at 340 nm was detected at 37°C in 1 min intervals over a period of 20 min, enzyme activity was calculated from the respective slopes.

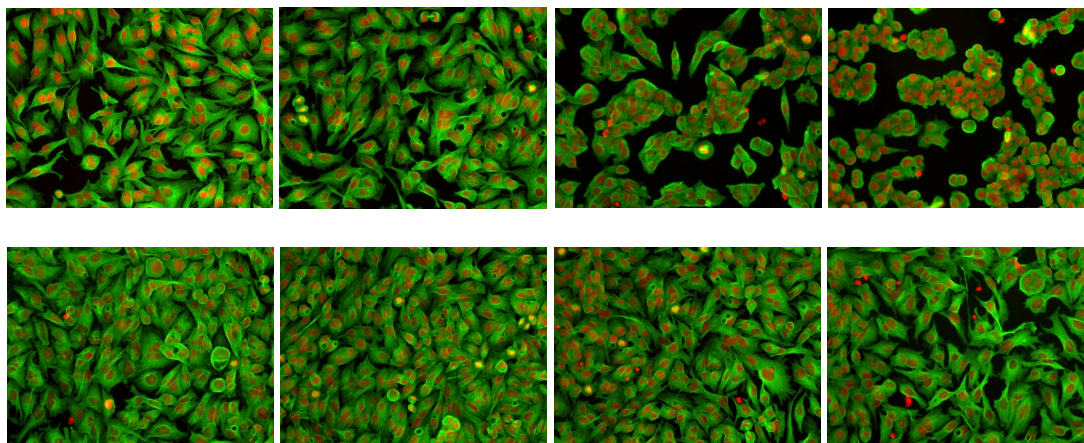


**Fig. S20.** Morphology of HepG2 treated with **(4cc)** (top), with **(4oc)** (mid) and quantification of the assay (bot) (0  $\mu$ M, 32  $\mu$ M, 125  $\mu$ M, 500  $\mu$ M). Human hepatoma HepG2 cells were propagated and maintained in DMEM (high glucose), supplemented with 10 % FBS, 25 U/ml penicillin and 25  $\mu$ g/ml streptomycin. 96-well plates were coated with 50  $\mu$ g/ml poly-L-ornithine (PLO) and 1  $\mu$ g/ml fibronectin over night at 37°C. Following a washing step of the coated plates with water, 30.000 cells/well were seeded and grown for 1 day. Then, the cells were treated with the respective compounds for additional 48 h. For visualization of cell morphology, cells were fixed with 4% paraformaldehyde for 20 min at RT, permeabilized with 0.2% Triton X-100, washed, and blocked with 1% BSA (Calbiochem, San Diego, CA) in PBS for 1 h. HepG2 were stained with a monoclonal anti- $\alpha$ -tubulin antibody (Sigma; 1:1000)

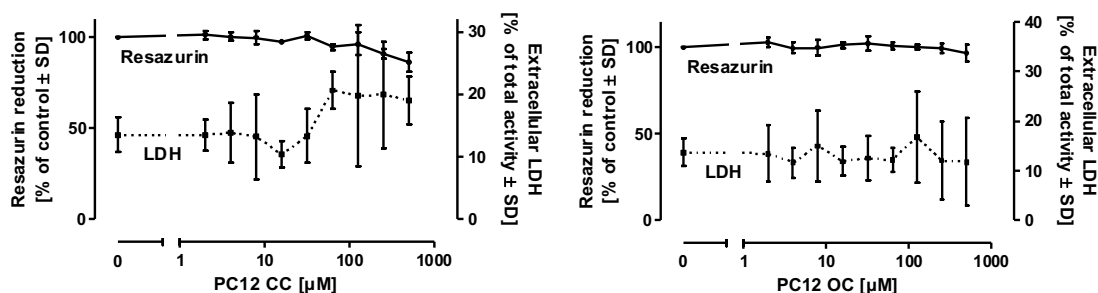


**Fig. S21.** Resazurin metabolization assay and Lactate dehydrogenase (LDH) release assay for the treatment of HepG2 with **(4cc)** (left) and **(4oc)** (right).

Resazurin metabolization assay: Resazurin (Sigma) was added to the cell culture medium in a final concentration of  $5 \mu\text{g/ml}$ , fluorescence was measured after 60 min ( $\lambda_{\text{ex}}=530 \text{ nm}$ ;  $\lambda_{\text{em}}=590 \text{ nm}$ ). Lactate dehydrogenase (LDH) release assay: LDH activity was detected separately in the supernatant and cell lysate. Following separation of the supernatants, cells were lysed in PBS / 0.5% Triton X-100 for  $> 60 \text{ min}$ . The percentage of LDH released was calculated as  $100 \times \text{LDH}_{\text{supernatant}} / \text{LDH}_{\text{supernatant} + \text{lysate}}$ . For the enzymatic assay,  $20 \mu\text{l}$  of sample was combined with  $180 \mu\text{l}$  of reaction buffer containing NADH ( $100 \mu\text{M}$ ) and sodium pyruvate ( $600 \mu\text{M}$ ) in sodium phosphate buffer adjusted to pH 7.4 by titration with  $\text{K}_2\text{HPO}_4$  ( $40 \text{ mM}$ ) and  $\text{KH}_2\text{PO}_4$  ( $10 \text{ mM}$ ). Absorption at  $340 \text{ nm}$  was detected at  $37^\circ\text{C}$  in 1 min intervals over a period of 20 min, enzyme activity was calculated from the respective slopes.



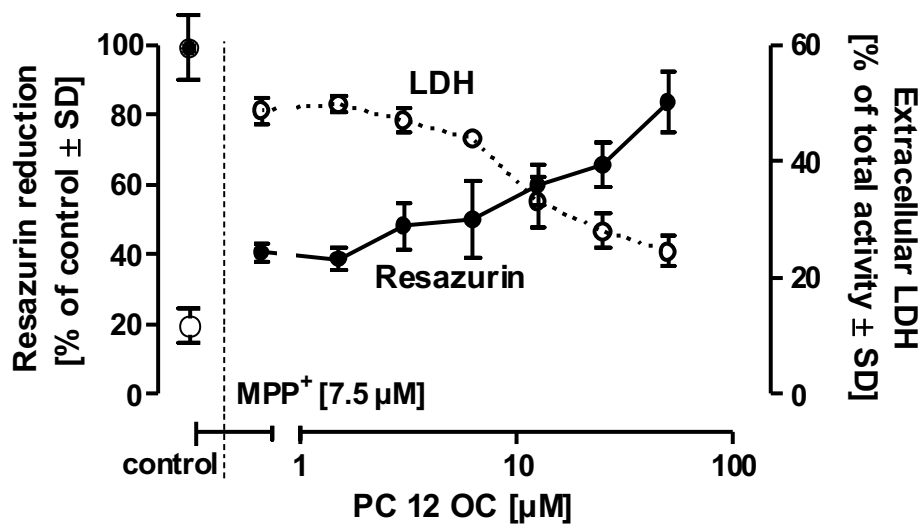
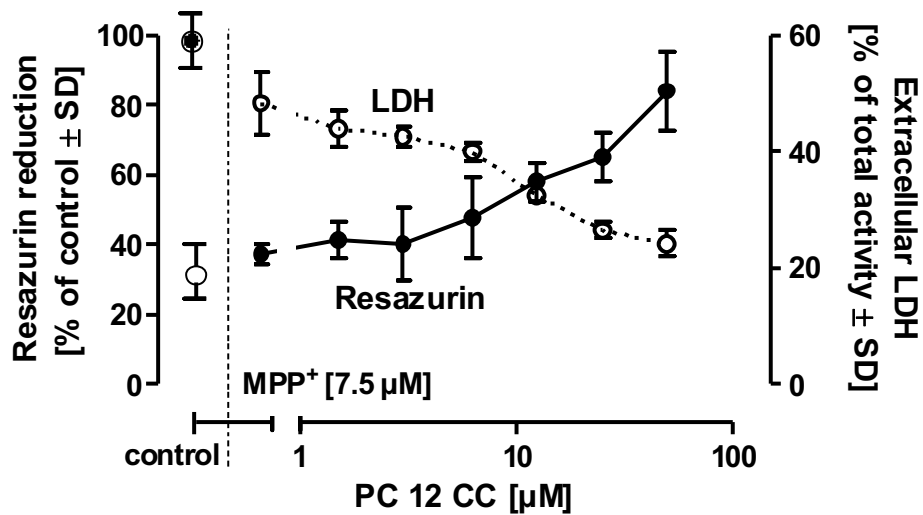


**Fig. S22.** Resazurin metabolism assay and Lactate dehydrogenase (LDH) release assay for the treatment of LUHMES with (**4cc**) and partially open cage compound (**4oc**) and MPP+.<sup>5-6</sup>

## References.

1. Farn, R. J.; Editor, *Chemistry and Technology of Surfactants*. Blackwell Publishing Ltd.: 2006; p 315 pp.
2. Demus, D.; Goodby, J.; Gray, G. W.; Spiess, H. W.; Vill, V., *Handbook of Liquid Crystals, Volume 2A: Low Molecular Weight Liquid Crystals I*. Wiley-VCH: 1998; p 490 pp.
3. Choi, H. S.; Kim, J. W.; Cha, Y. N.; Kim, C., A Quantitative Nitroblue Tetrazolium Assay for Determining Intracellular Superoxide Anion Production in Phagocytic Cells. *J. Immunoass. Immunoch.* **2006**, *27* (1), 31-44.
4. Schildknecht, S.; Pape, R.; Müller, N.; Robotta, M.; Marquardt, A.; Bürkle, A.; Drescher, M.; Leist, M., Neuroprotection by Minocycline Caused by Direct and Specific Scavenging of Peroxynitrite. *Journal of Biological Chemistry* **2011**, *286* (7), 4991-5002.
5. Schildknecht, S.; Pörtl, D.; Nagel, D. M.; Matt, F.; Scholz, D.; Lotharius, J.; Schmiege, N.; Salvo-Vargas, A.; Leist, M., Requirement of a Dopaminergic Neuronal Phenotype for Toxicity of Low Concentrations of 1-methyl-4-phenylpyridinium to Human Cells. *Toxicology and applied pharmacology* **2009**, *241* (1), 23-35.
6. Scholz, D.; Pörtl, D.; Genewsky, A.; Weng, M.; Waldmann, T.; Schildknecht, S.; Leist, M., Rapid, Complete and Large-scale Generation of Post-mitotic Neurons from the Human LUHMES Cell Line. *Journal of neurochemistry* **2011**, *119* (5), 957-971.